Fracture Network Interpretation Through High Resolution Velocity Models: Application to The Geysers Geothermal Field

Tayeb A. Tafti and Fred Aminzadeh

University of Southern California, Los Angeles CA, USA

Keywords

Geothermal reservoir, fracture, microseismic, The Geysers, tomographic inversion, Poisson's ratio

ABSTRACT

Steam at many geothermal fields including The Geysers is produced from a network of fractures in crystalline rocks. Some of these fracture networks have been created by injecting cool water into the hot rock while others are natural tectonic fractures associated with the nearby San Andreas Fault plate boundary. Due to very low permeability of the formation matrix in The Geysers reservoir, production depends on the presence of these natural or induced fractures. Hence, locating and characterizing fracture networks is of vital importance. During injection of water, newly created fractures induce microseismic events. A small number of triggered seismicity could also be created from fault failures. Although pinpointing the locations of microseismic events is a useful characterization tool, we go beyond the simple locations identification to characterize fractures more reliably.

We apply tomographic inversion to the microseismic data to obtain high resolution compressional (P) and shear (S) wave seismic velocity volumes of the area of interest. We show how these velocity models can help us in characterization process. In addition, we demonstrate how P and S velocity volumes can be integrated with each other or with other data sets to derive additional reservoir property volumes. Such additional information can then be used to optimize injection schedule, improve the production rates or locating the potential zones for enhanced geothermal systems.

1. Introduction

In the last decade, many authors have published their research about using the microseismic activity in order to interpret the fracture height, length, azimuth, zonal coverage, and fracture complexity in terms of a simple, planar fracture, or a complex fracture network. They have also tried to correlate production data with the dimensions of the microseismic clouds and volume estimates based on the density of microseismic events (Albright, 1982; Brady et al., 1994; Rutledge et al., 1998; Phillips et al., 1998; Fisher et al., 2004; Downie et al., 2009; Barree et al., 2002; Xu and Calvez, 2009; Warpinski et al., 2005; Tezuka et al., 2008). For instance, Tezuka (2000); Moriya et al. (2000); Rowe et al. (2002); Rutledge (2003) used both focal mechanism analysis as well as microseismic multiplet analysis to delineate the reservoir structure and examine the associated permeability creation later. Grechka and Mazumdar (2010); Hummel and Shapiro (2011) predicted the permeability and production of hydraulically fractured reservoirs from microseismic data using diffusivity equation, microseismic events cloud geometry, and their temporal changes. Finally, Charlety et al. (2006) used 4D tomographic inversion in Soultz EGS site to evaluate the stimulation process. Moreover, various approaches have been used to characterize the fracture network at The Geysers including geologic mapping (Hebein, 1986; Sternfeld, 1989), outcrop analysis (Sammis et al., 1991), core analysis (Nielson et al., 1991), microseismic analysis (Tafti and Aminzadeh, 2011), fuzzy clustering (Aminzadeh et al., 2010), and shear wave splitting (Elkibbi, 2005). In this article, we demonstrate how we can interpret the high resolution velocity models, extracted from microseismic data, to characterize the fracture network at The Geysers. We try to obtain the fundamental understanding of the relationship between seismic velocity models (both shear and compressional wave) and reservoir properties to accomplish this task.

Effective, reliable, and accurate characterization of the fracture network especially their complex fracture system at this site necessitates fundamental under-standing of the geophysical and geomechanical properties of the reservoir rocks and fracture systems. Geophysical and geomechanical anomalies in the reservoirs can be associated to various features of the reservoir such as porosity, fracture density, salinity, saturation, tectonic stress, fluid pressures, and lithology. Therefore, a more tedious approach is required to accurately interpret these anomalies. We will rely on realistic assumptions and data such as lithology logs, laboratory measurement of rock properties and other information about microseismic data to find the best possible solution to characterize the

fracture network. The dataset used for this study include velocity models provided by the Lawrence Berkeley National Laboratory (LBNL) extracted from 2004 micro-seismic events (Boyle et al., 2011; Hutchings et al., 2011). Then the resolution of these velocity models enhanced using the method described in our previous publication, (Tafti and Aminzadeh, 2011).

2. Fracture Mapping Using Seismic Velocity Models

Having both compressional and shear wave velocity models, it is possible to define most of the elastic rock properties uniquely (Tokosoz and Johnson, 1981). These velocities are approximately related to the square root of its elastic properties and inversely related to its inertial properties.

$$V(approx.) = \sqrt{\frac{Elastic\ \ property}{Inertial\ \ property}} \qquad (1)$$

For instance in Rock materials, V_P and V_S are defined in equation 2 and 3.

$$V_P = \sqrt{\frac{B + \frac{4\mu}{3}}{\rho}} \qquad (2)$$

$$V_S = \sqrt{\frac{\mu}{\rho}} \qquad (3)$$

Where ρ is density (an inertial property), B is bulk modulus and μ is shear modulus. Normal stress (σ_n), hydrostatic stress (σ_h), and Poisson's ratio can also be described in term of these seismic velocities[1] (Tokosoz and Johnson, 1981).

$$\sigma_n^2 = \frac{V_S^2(3V_P^2 - V_S^2)}{(V_P^2 - V_S^2)} \qquad (4)$$

$$\sigma_h^2 = V_P^2 - \frac{4}{3}V_S^2 \qquad (5)$$

$$\upsilon = \frac{V_P^2 - 2V_S^2}{2(V_P^2 - V_S^2)} \qquad (6)$$

After calculating the necessary property volumes, we need to define a framework to relate these geophysical and geomechanical properties to fractured reservoir properties. Martakis et al. (2006) generalized that V_P shows the structural details of the reservoir and V_P/V_S illuminates lithological details. However, we and many other authors believe that many factors affect these velocities in all scales such as porosity (Wyllie et al., 1956; Wyllie and Gregory, 1958; Berry-man et al., 2002), fractures (Berge et al., 2001; Berryman and Wang, 2000), pore pressure, and saturation (Nur and Simmons, 1969; Berryman et al., 2002).

White (1975) reported an increase in V_P with saturation, while V_S remained unchanged, while Figure 1c clearly shows that saturation[2] has small or no effect on the V_P but we can observe modest reduction in the V_S at The Geysers' core measurement. Table 1 explains the effect of saturation resulting from three different scenarios: fluid density, fluid compressibility, and shear weakening. Saturation raises the V_P / V_S and reduces V_S in two of these scenarios, with little resulting effect on V_P. Hence, we can conclude that high V_P / V_S anomalies associated with low V_S anomalies are saturation anomalies. In the other hand, low V_P / V_S anomalies associated with low V_P are caused from another phenomenon such as lithology or fracture density variations (Boitnott, 2003).

Table 1. Effect of saturation on seismic velocities (Boitnott, 2003).

Mechanism	Description	VP	VS	VP /VS
Fluid Density	Saturation causes a increase in bulk density, resulting in a decrease in velocities	Decreases	Decreases	No Change
Fluid Compressibility	Adding an incompressible fluid stiffens the pores to compression, increasing the bulk modulus of the rock	Increases	No Change	Increases
Shear Weakening	The presence of liquid water acts to weaken the shear modulus of the rock.	Decreases	Decreases	Increases

Figure 1b shows V_P is negatively correlated with porosity. It is notable that different lithologies demonstrate dissimilar trends.

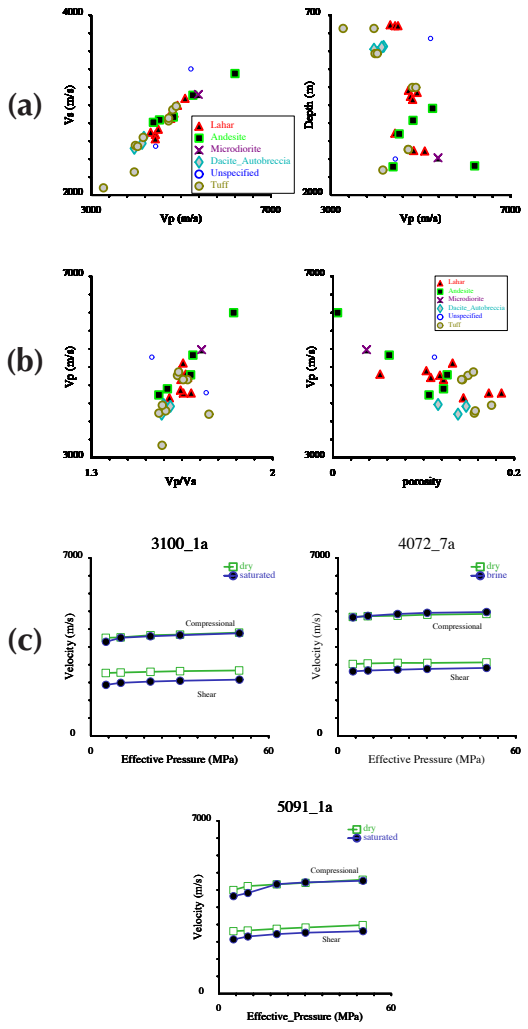

Figure 1. Seismic velocities for various rock samples versus (a) depth for dry samples, (b) porosity for dry samples, (c) effective confining pressure for dry and brine saturated rocks (Boitnott, 2003).

Some with wide range of velocities confined in narrow range of porosities, some have wide range of porosities confined in narrow range in velocities, and some show a strong correlation of velocities with porosities. Charlety et al. (2006) also reported decrease in V_P with porosity using velocity and flowrate correlation. In conclusion, velocities are sensitive to porosity and rock-type, but other factors such as textural and mineralogic variations can also impact this behavior. Figure 1c illustrates that seismic velocities are insensitive to pressure, persisting to high effective pressures. Charlety et al. (2006) reported that reservoir pore pressure can reduce the V_P in field scale measurement.

Furthermore, Effective medium theories[3] would suggest that low V_P and V_S indicate highly fractured regions, while high V_P and V_S may indicate unfractured regions (Berge et al., 2001). Increasing depth may close fractures and cracks which can increase seismic velocities (Figure 1a illuminates no clear separation between lithologies and no apparent signature with depth in core analysis where we do not have overburden pressure to close the fractures). In addition, Charlety et al. (2006) reported that the porosity created from microcracks, increase fluid saturation, and raise the pore pressure. They reported the slow increase in seismic velocity with time which related to the cooling of the rock by the injected colder fluid and the increase in water saturation. But, he observed overall reduction in the P-wave velocity by creating microcracks in the reservoir.

Figure 2a illustrates the behavior of a fracture under a two-dimensional stress condition. Three types of stresses typically act on the fracture surface, which are defined as: normal stress (σn), shear stress, and static frictional stress. Each of these states of stress can cause associated fracture mode as shown in Figure 2b. Figure 2a also shows the state before pore pressure (p) increase caused by injection from stimulation in hydraulic fracturing or the initial contact of water with new planes of weakness. Fluid injection reduces the effective normal stress and raises the pore pressure which depreciates the peak stress that the interface can support. Hence, at some level of pore pressure increase, shear slip may occur once the peak frictional stress becomes smaller than the shear stress. In addition, reduced effective stress may also cause fracture dilation. We can use the effective normal stress as an index for fracture opening[4] which is essential for fluid movement and production. We can also use the hydrostatic stress as an indicator of pore pressure. Tezuka (2000); Ameen (2003) also reported that shear slippage along pre-existing fractures or flaws caused by pore pressure increase can create fluid flow pathways for production. They hypothesized that since the shear failure fractures have the associated condition where Coulomb failure is reached for smallest pore pressure increase, this type of fractures mainly contribute towards fluid production and the distribution of these favorably oriented pre-existing fractures and their interaction with the regional stress field strongly controls the growth direction of the reservoir.

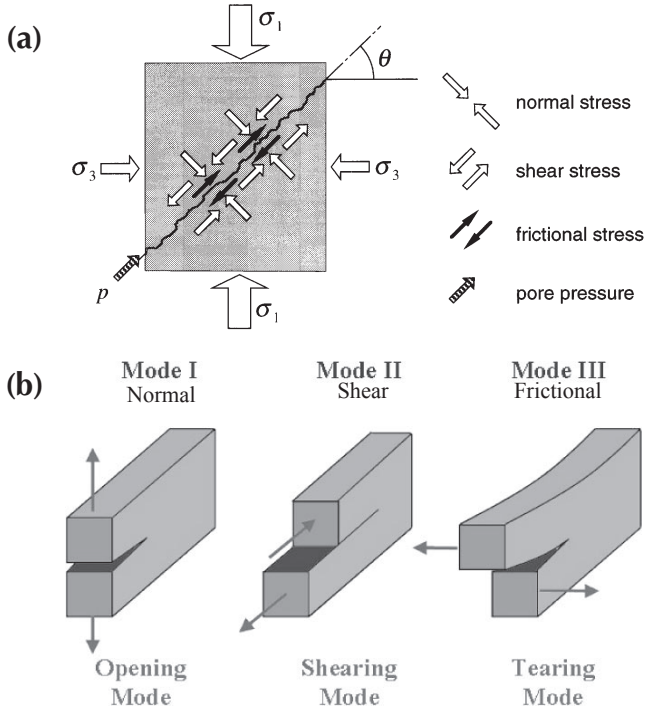

Figure 2. (a) Diagram illustrating the fracture subjected to dimensional stress condition (Tezuka, 2000), (b) associated fracture mode to different states of stress (Rountree et al., 2002).

In summary, closing of small cracks due to pressure with depth, increase in overburden pressure, and cementation are some causes of increase in seismic velocity. Fracturing, chemical alteration, extreme temperature gradient with depth, pore pressure, and porosity are main causes for reduction in velocities. Fluid saturation has different effects but overall, has little effect on V_P, reduces V_S and enhances V_P / V_S with a higher degree of impact on V_P / V_S and Poisson's ratio. For a highly fractured region, we expect low V_P and V_S while high V_P and V_S may indicate unfractured regions. In addition, both hydrostatic stress and normal stress distribution can be used to identify and delineate the fractured areas from unfractured ones.

3. Results and Discussion

We consider two different horizons in The NW Geysers geothermal field to test our methodology. The first horizon is located in the normal temperature reservoir (NTR) where the injection and production wells have been completed. Existing fracture network, within this zone, has main role in production of steam. Our aim in this horizon is locating and characterizing the fracture network. The second horizon is the area 1500 ft below the completion points within high temperature zone (HTZ) where we have no production. Our goal here is finding zones where the fracture network propagates in order to create an enhanced geothermal system. Figures 3 shows V_P, V_S, and V_P /V_S on these two horizons in the NW Geysers. High V_P /V_S anomalies associated with low V_S anomalies are saturation anomalies. On the other hand, high V_P /V_S anomalies associated with high V_P are caused by other phenomena such as lithology effects. Finally, it is reasonable to assume that low V_P / V_S anomalies associated with low V_P anomalies are fracture related anomalies. Based on the identified framework, we can identify highly fractured zones of interest by interpreting the observed velocity anomalies. As per our discussion, we can identify the area below and around SB27 and DX23 have the highest fracture density. On the other hand, area below and around LF2 and CMHC2 have the lowest fracture density within this horizon. Moreover, we can successfully locate the propagated fracture network in the high temperature zone below the SB27 and DX77 wells.

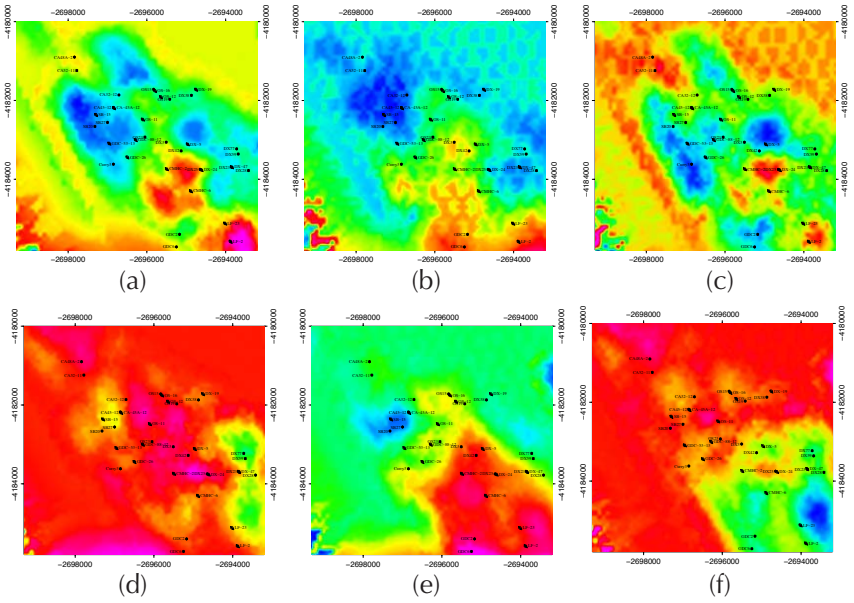

Figure 3. NTR horizon at The NW Geysers (a)V_P , (b) V_S, (c)V_P /V_S, HTZ horizon (d)V_P , (e) V_S, (f)V_P /V_S.

Figure 4 clearly shows that Poisson's ratio anomalies follow a similar trend when compared with V_P /V_S anomalies and this is a good indicator of fluid saturation. Reduction in normal stress indicates the areas where fractures are open to provide sufficient permeability along with low velocity anomalies and this acts as a further validation that the identified anomalies are fracture related and not from lithology or other phenomena.

3.1 Tomographic Inversion Versus Shear Wave Splitting

Comparing shear wave splitting results and tomographic inversion results can eliminate errors that are common when they are analyzed individually. This work is aimed at integrating our results with those by Elkibbi (2005). Table 2 illustrates station numbers and their corresponding names.

Table 2. Seismic station numbers and their corresponding names at The NW Geysers.

Station Number	Station Name
S1	STY
S2	INJ
S3	BUC
S4	SQK
S5	DRK
S6	FUM
S7	JKR
S8	DXR
S9	CLV

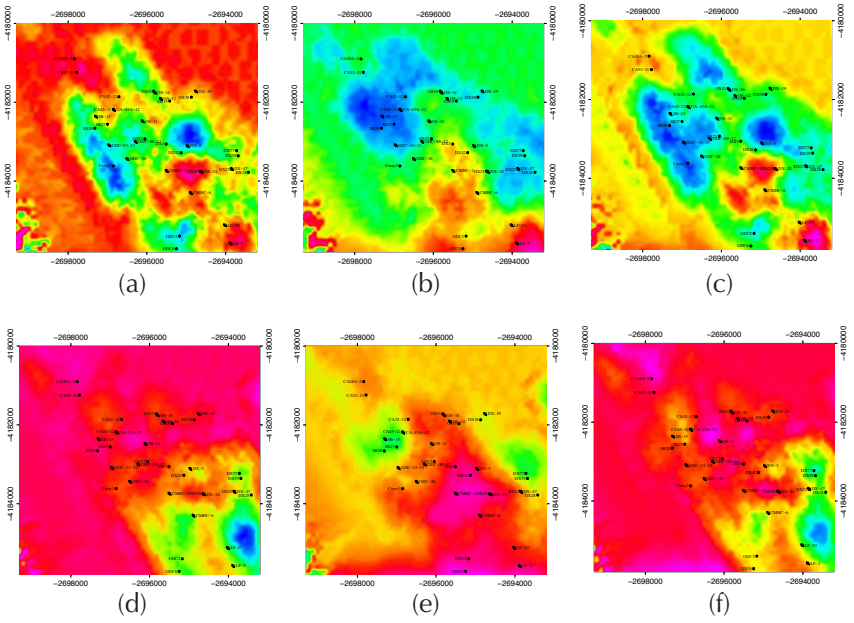

Figure 4. NTR horizon at The Geyser (a)Poisson's ratio, (b) Normal stress, (c)Hydrostatic stress, HTZ horizon at The Geyser (d)Poisson's ratio, (e) Normal stress, (f)Hydrostatic stress

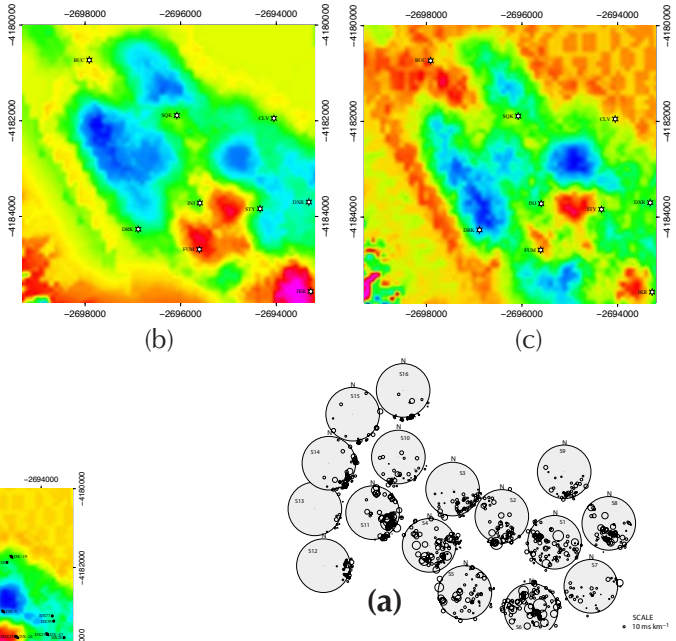

Figure 5. (a) Fracture density result from shear wave splitting (Elkibbi, 2005), (b) V_P , (c) V_P /V_S in the NW Geysers.

Elkibbi (2005) indicated that time delays observed between the slow and fast shear waves at The NW Geysers varies between 8 to 40 ms/Km. As seen in figure 5, cross plotting Elkibbi's results with those we have obtained can help in spatial interpretation of the fracture zone densities. Regions with low V_P and V_P /V_S anomalies along with high time delays should indicate zones having high fracture densities. Our comparative analysis indicates that our interpretation of high fracture density zones within the reservoir correlate well with those obtained by Elkibbi.

In addition, figure 6 demonstrates that stations near Squaw Creek Fault Zone (S4, S5, S6, and S11)

have higher fracture density than others. This is consistent with normal stress distribution which indicates open fractures. On the other hand, high time delays occur at stations S1, S2, S3, and S8 which indicates that this area may also have higher fracture intensity than western stations but they show a higher degree of consistency with Poisson's ratio distribution instead of normal stress. Hence, it can be hypothesized that the time delays observed in this particular case are due to fluid saturations or other fluid properties.

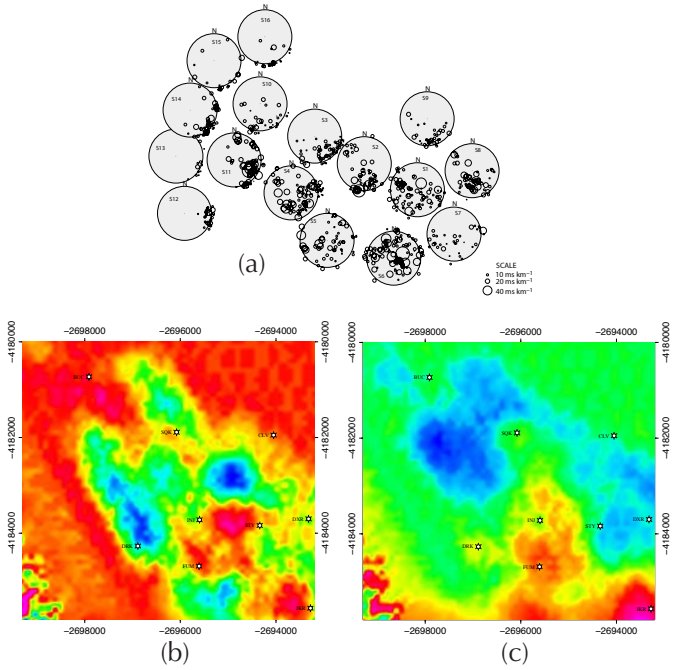

Figure 6. (a) Fracture density result from shear wave splitting (Elkibbi, 2005), (b) Poisson's ratio, (c) Normal stress in the NW Geysers.

3.2 *Tomographic Inversion Versus Production/Injection Data*

Figure 7 validates those regions with higher fracture density anomalies (such as low V_P and low normal stress as discussed) correlate with higher steam production with relatively low water injection levels. This is consistent with our hypothesis and theory from the preceding discussions. On the other hand, lower Poisson ratio or lower V_P /V_S are not self-indicative of higher fracture intensity and these anomalies could be associated with other phenomena such as degree of fluid saturation or fluid type.

4. Summary

In summary, after joint interpretation of velocity, Poisson's ratio, normal stress, and hydrostatic stress, we could identify the NW trend of the regional fracture network and the zones having higher fracture density within the NTR. Within the HTZ, it is possible to identify fracture networks that penetrate the NTR and move into the HTZ based on major variations in V_P, hydrostatic pressure and normal stress anomalies. We have also demonstrated how the integration of shear wave splitting, production-injection data and velocity modeling can help us clarify our hypothesis which relates the velocity, stress anomalies with the propagating fracture

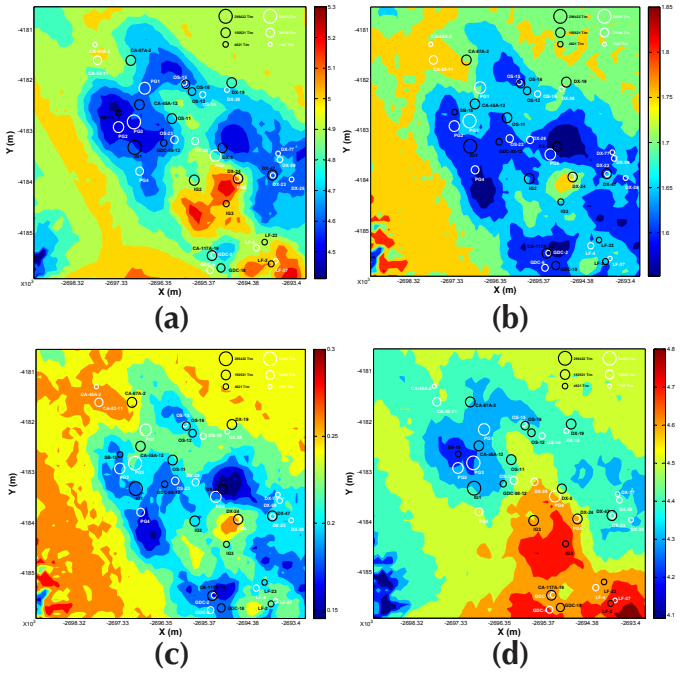

Figure 7. NTR horizon at The NW Geysers, (a)V_P , (b) V_P /V_S, (c) Poisson's ratio (d) Normal stress, with production/injection data superimposed(Production: White, Injection: Black).

network. Furthermore, they provide a useful tool for long-term improvements to well spacing plan, well design, and completion design at The Geysers. This eliminates the errors in locating the fractured areas and can help us in targeting the stimulated area for future development plans.

5. Acknowledgements

This work is supported by the Department of Energy ARRA GRANT10379400 to University of Southern California. We would like to acknowledge the developers of Zmap, Matlab, SGeMS and Opendtect for providing us with academic licenses. We would also like to thank Ernie Majer, Stephen Jarpe and Katie Boyle from LBNL for their expert advice and support providing the initial velocity models and catalogs. We are also grateful to Muhammad Sahimi and Charles Sammis, and Debotyam Maity from USC for their continued collaboration. We have also benefited from interactions and many useful discussions with Joseph Beall and Mark Walter from Calpine.

6. References

Albright, J., 1982. Acoustic emissions as a tool for hydraulic fracture location: Experience at the fenton hill hot dry rock site. Old SPE Journal.

Ameen, M., 2003. Fracture and in situ stress characterization of hydrocarbon reservoirs. The Geological Society, London.

Aminzadeh, F., Tafti, T. A., Maity, D., 2010. Characterizing fractures in the geysers geothermal field using soft computing. GRC Transactions 34, 1193– 1198.

Barree, R., Fisher, M., Woodroof, R., 2002. A Practical Guide to Hydraulic Fracture Diagnostic Technologies. In: SPE Annual Technical Conference and Exhibition.

Berge, P., Hutchings, L., Wagoner, J., 2001. Rock Physics Interpretation of P-Wave Q and Velocity Structure, Geology, Fluids and Fractures at the Southeast Portion of The Geysers Geothermal Reservoir. Geothermal Res. Council, Transactions 14, 1–21.

Berryman, J. G., Berge, P. a., Bonner, B. P., 2002. Estimating rock porosity and fluid saturation using only seismic velocities. Geophysics 67 (2), 391.

Berryman, J. G., Wang, H. F., 2000. Elastic wave propagation and attenuation in a double-porosity dual-permeability medium. Science 37, 63–78.

Boitnott, G., 2003. Core analysis for the development and constraint of physical models of geothermal reservoirs. Tech. rep., New England Research.

Boyle, K., Majer, E., Jarpe, S., Saltiel, S., 2011. Investigation of an aseismic 'doughnut hole' region in the northwest geysers, california. Geothermal Resources Council Transactions.

Brady, J., Withers, R., Fairbanks, T., Dressen, D., Sep. 1994. Microseismic monitoring of hydraulic fractures in prudhoe bay. Proceedings of SPE Annual Technical Conference and Exhibition, 387–398.

Charlety, J., Cuenot, N., Dorbath, C., Dorbath, L., Oct. 2006. Tomographic study of the seismic velocity at the Soultz-sous-Forˆets EGS/HDR site. Geothermics 35 (5-6), 532–543.

Downie, R., Le Calvez, J., Kerrihard, K., 2009. Real-Time Microseismic Monitoring of Simultaneous Hydraulic Fracturing Treatments in Adjacent Horizontal Wells in the Woodford Shale. cspg.org, 484–492.

Elkibbi, M., 2005. The Geysers geothermal field: results from shear‐wave splitting analysis in a fractured reservoir. Geophysical Journal International, 1024–1035.

Fisher, M., Heinze, J., Harris, C., Wright, C., Dunn, K., 2004. Optimizing horizontal completion techniques in the Barnett shale using microseismic fracture mapping. In: SPE Annual Technical Conference and Exhibition.

Grechka, V., Mazumdar, P., 2010. Predicting permeability and gas production of hydraulically fractured tight sands from microseismic data. Geophysics 75 (1).

Hebein, J., 1986. Reservoir fracturing in the geysers hydrothermal system: Fact or fallacy? In: Proceedings, 11th Stanford Workshop on Geothermal Reservoir Engineering. pp. 43–50.

Hummel, N., Shapiro, S., 2011. Nonlinear diffusion estimates from hydraulic fracturing of shales. SEG Annual Meeting, 1544–1549.

Hutchings, L., Jarpe, S., Boyle, K., Viegas, G., Majer, E., 2011. Inexpensive , Automated Micro-Earthquake Data Collection and Processing System for Rapid , High-Resolution Reservoir Analysis. GRC Transactions 35, 1679– 1685.

Martakis, N., Kapotas, S., Tselentis, G., Others, 2006. Integrated passive seismic acquisition and methodology. Case studies. Geophysical prospecting 54 (6), 829–847.

Moriya, H., Nakazato, K., Niitsuma, H., Baria, R., 2000. STUDY OF MICROSEISMIC DOUBLET/MULTIPLET FOR EVALUATION OF SUBSURFACE FRACTURE SYSTEM IN SOULTZ HDR FIELD. In: Proc. World Geothermal Congress 2000. pp. 3807–3812.

Nielson, D., Walters, M., Hulen, J., 1991. Fracturing in the northwest geysers, sonoma county, california. Transactions, Geothermal Resources Council 15, 27–33.

Nur, A., Simmons, G., 1969. The effect of saturation on velocity in low porosity rocks. Earth and Planetary Science Letters 7 (2), 183–193.

Phillips, W., Rutledge, J., Fairbanks, T., Gardner, T., Miller, M., Maher, B., 1998. Reservoir fracture mapping using microearthquakes: Two oilfield case studies. SPE Reservoir Evaluation and Engineering 1 (2), 114–121.

Rountree, C. L., Kalia, R. K., Lidorikis, E., Nakano, A., Van Brutzel, L., Vashishta, P., Aug. 2002. A TOMISTIC A SPECTS OF C RACK P ROPAGATION IN B RITTLE M ATERIALS : Multimillion Atom Molecular Dynamics Simulations. Annual Review of Materials Research 32 (1), 377–400.

Rowe, C., Aster, R., Phillips, W., Jones, R., 2002. Using automated, high-precision repicking to improve delineation of microseismic structures at the Soultz geothermal reservoir. Pure and Applied 159, 563–596.

Rutledge, J., 2003. Hydraulic stimulation of natural fractures as revealed by induced microearthquakes, Carthage Cotton Valley gas field, east Texas. Geophysics.

Rutledge, J., Phillips, W., House, L., Zinno, R., 1998. Microseismic mapping of a cotton valley hydraulic fracture using decimated downhole arrays. Proc. 68th Ann. Mtg., SEG, 338–341.

Sammis, C. G., An, L. J., Ershaghi, I., 1991. Fracture patterns in graywacke outcrops at the geysers geothemral field. In: Sixteenth Workshop on Geothermal Reservoir Engineering. Stanford.

Sternfeld, J., 1989. Lithologic influences on fracture permeability and the distribution of steam in the northwest geysers steam field, sonoma county, california. GRC Trans 13, 473–480.

Tafti, T. A., Aminzadeh, F., 2011. Fracture Characterization at The Geysers Geothermal Field using Time Lapse Velocity Modeling , Fractal Analysis , and Microseismic Monitoring. Geothermal Resources Council (GRC) Transactions 35, 547–551.

Tezuka, K., Apr. 2000. Stress estimated using microseismic clusters and its relationship to the fracture system of the Hijiori hot dry rock reservoir. Engineering Geology 56 (1-2), 47–62.

Tezuka, K., Kamitsuji, R., Tamagawa, T., 2008. Fractured Reservoir Characterization Incorporating Microseismic Monitoring and Pressure Analysis During Massive Hydraulic Injection. In: International Petroleum Technology Conference.

Tokosoz, M. N., Johnson, D. H., 1981. Seismic wave attenuation. Society of Exploration Geophysicists.

Warpinski, N., Kramm, R., Heinze, J., Waltman, C., 2005. Comparison of single-and dual-array microseismic mapping techniques in the Barnett shale. In: SPE Annual Technical Conference and Exhibition. October.

White, J., 1975. Computed seismic speeds and attenuation in rocks with partial gas saturation. Geophysics 40 (2), 224.

Wyllie, M., Gregory, A., 1958. An experimental investigation of factors affecting elastic wave velocities in porous media. Geophysics 23 (3), 459–493.

Wyllie, M., Gregory, A., Gardner, L., 1956. Elastic wave velocities in heterogeneous and porous media. Geophysics 21 (1), 41.

Xu, W., Calvez, J. L., 2009. Characterization of Hydraulically-Induced Fracture Network Using Treatment and Microseismic Data in a Tight-Gas Sand Formation: A Geomechanical Approach. SPE Tight Gas Completions.

[1] Modulus are in GPa $=1.45 \times 10^5$psi and velocities are in km/s.

[2] Brine saturation

[3] Physical models that describe the macroscopic properties of a medium based on the properties and the relative fractions of its components.

[4] The fracture walls become completely separated when the effective normal stress become zero.